Testing of The NASA GSFC MEMS Colloidal Thruster

IEPC-2005-306

Eric H. Cardiff[*], Brad Degen[†], Abraham Grindle[‡], Brian Jamieson[§], Loral O'Hara[**], Kevin Pearce[††], and Patrick Roman[‡‡]
NASA Goddard Space Flight Center, Greenbelt, MD, 20771, USA

An enabling technology for upcoming NASA formation flight missions is the colloidal thruster. A MEMS version of the colloidal thruster has been developed to operate over a wide thrust range. The NASA GSFC MEMS colloidal thruster has solved the problem of electrical breakdown to permit the integration of the electrode on top of the emitter by a novel MEMS fabrication technique. Devices have been successfully fabricated and operated. An experimental setup was used to test the devices with both optical and Time Of Flight diagnostics, and preliminary results of these tests are presented here.

Nomenclature

I	=	current
L	=	distance between the emitter and the collector
$\dot{m}$	=	mass flow rate
t_F	=	time of flight
q/m	=	charge to mass ratio of the colloidal droplets
T	=	thrust
V_A	=	acceleration potential (= V_N-V_S)
V_N	=	needle voltage
V_S	=	stopping potential

I.   Introduction

A number of potential NASA missions require very precise attitude control with thrusts as low as 0.1 µN. Many of these upcoming missions use interferometers as part of the instrumentation, and the science results are therefore sensitive to the position of the spacecraft with respect to one another. Some of these potential missions are the Laser Interferometer Space Antenna (LISA), Micro-Arc second X-ray Imaging Mission (MAXIM), Space Interferometer Mission (SIM), Constellation-X, and Terrestrial Planet Finder (TPF). "Drag-free" missions also require similar propulsion systems to eliminate noise from gravitational disturbances. An example of this type mission is Gravity Probe B. These missions could be enabled by a MEMS colloidal thruster. A colloidal thruster is capable of providing the required thrust, but the state of the art devices, such as those that will fly on ST-7, are large and massive compared to potential new miniaturized systems.

---

[*] Propulsion Engineer, Propulsion Branch, Eric.H.Cardiff@nasa.gov.
[†] Intern, Propulsion Branch, bdegen@wpi.edu.
[‡] Intern, Propulsion Branch, grindlea@slu.edu.
[§] MEMS Engineer, Detector Systems Branch, Brian.G.Jamieson@nasa.gov.
[**] Intern, Propulsion Branch, loral.ohara@gmail.com.
[††] Intern, Propulsion Branch, spree15@wpi.edu.
[‡‡] MEMS Engineer, Detector Systems Branch, proman@pop500.gsfc.nasa.gov.

II. The NASA GSFC MEMS Colloidal Thruster

A colloidal thruster has been developed at NASA GSFC to enable these missions. Developing the thruster as a Micro-ElectroMechanical Systems (MEMS) device on a silicon wafer allows large numbers of arrays to be manufactured cheaply and rapidly, and will allow greater emitter density to be used, thereby extending the thrust range. It is an internally wetted design to simplify spacecraft integration issues. In addition, the colloidal thruster is particularly well suited to micro-fabrication, as the associated smaller dimensions reduce the voltages required for operation.

The primary challenge in designing a MEMS electric thruster is the development of insulation between the accelerating electrodes and the emitter[1]. Attempts by other researchers to develop this type of thruster have failed due to electrical breakdown of the insulation[2], or have required complicated designs[3].

The thruster described here was built entirely at Goddard Space Flight Center, using novel MEMS fabrication techniques. The insulation was described previously in Cardiff *et al.*[4] The fabrication of the emitters was performed via the following steps:

- An insulation pattern was etched on the top surface of the silicon wafer, consisting of concentric circular columns that were 10 μm wide by 70 microns deep via Deep Reactive Ion Etch (DRIE).
- The emitter through hole was patterned and etched through the bottom of the wafer.
- The area around the emitter hole was masked off to prevent oxidation.
- The insulation comb structure was then oxidized via a long wet heat treatment to change the insulation columns into silicon dioxide.
- The silicon wafer was diced to separate the emitters.
- The electrodes were bonded to the insulation pattern of each emitter using a thin layer of adhesive on the electrodes.

III. Colloidal Thruster Theory

The colloidal thruster is an electrostatic propulsion technology. Thrust is produced by the electrostatic acceleration of small charged liquid droplets. The emitter has traditionally been a small hypodermic needle that is biased to a potential of several kilovolts. An electrode with an opposite electric potential is placed above this emitter needle. A conductive ionic solution present in the needle is pulled towards the electrode in a characteristic cone shape. This cone shape was first observed in 1914 by Zeleny[5]. Extensive work was done on colloid thrusters through the 1960's, but these thrusters required voltage on the order of 10 kV[6].

The fluid cone shape was comprehensively described and characterized by G. I. Taylor in 1965[7], and is therefore commonly referred to as a "Taylor cone". The Taylor cone is formed by the interaction of the electrostatic field and the surface tension. At a critical diameter of the cone, it becomes unstable and breaks down into a stream of individual droplets. Charge concentration at the fluid surface gives these droplets a net charge. Thrust is produced as these droplets are accelerated away from the emitter by the electric field.

A schematic of the traditional setup of a needle colloidal thruster is shown in Figure 1. The Space Technology 7 (ST-7) project uses this type of colloidal thruster, as fabricated by Busek Co., Inc. The ST-7 colloid thruster is composed of 8 thrusters arranged in 2 clusters, with 9 needles per thruster.

Figure 1. Traditional "needle" colloidal thruster.

IV. Experimental Setup

Testing was performed in the glass bell jar shown in Figure 2. All of the hardware is insulated from the stand and mounted on a Teflon plate. A vacuum flange is used as a propellant supply tank with pressurant gas (air) at atmospheric pressure. The propellant is delivered via a hypodermic tube and a Lee micro-valve. Propellant conductivities from 0.5 to 2 S/m were used for solutions with sodium iodide in formamide. The static voltage is applied from both a Bertran power supply (negative) and an EMCO power supply (positive). The high voltages are routed through an ISI vacuum flange rated to 6000 VDC. Images are obtained with a Mitutoyo microscope in vacuum and captured by a high-resolution black and white 2/3" CCD camera. The microscope focus changes slightly as pressure changes in the bell jar, but focus is readjusted by small displacements with a vacuum-rated Velmex positioning stage.
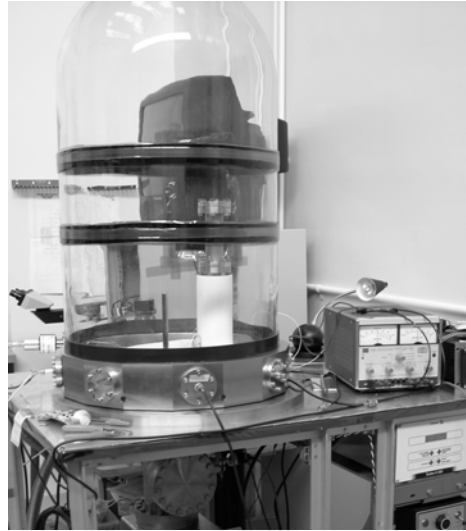
Figure 2. Picture of the test setup in the bell jar (monitor is located behind the bell jar).

Figure 2 shows the bell jar used for testing without the microscope. A closeup of the microscope is shown in Figure 3 (left). The mounting fixture for the electrode is located in the foreground, with the propellant tank (supported on a large Teflon insulator) in the background. The mounting system is used to translate the electrode directly into place over the emitter hole and attach, while remaining in the field of view of the microscope. Figure 3 (right) shows a closeup of the emitter mounting, with the electrode mounted on top of the insulation.

Figure 3. Closeup of the microscope and emitter positioning stage (left), and a closeup of the emitter and attached electrode(right).

The 29th International Electric Propulsion Conference, Princeton University,
October 31 – November 4, 2005

The emitter was primed by accurately controlling the amount of propellant allowed through the valve: enough propellant was allowed through the valve to fill the propellant feed tube and to form a liquid meniscus at the outlet of the emitter hole. This priming operation was performed in real time with the valve operator watching the video output of the microscope and pulsing the valve actuation circuit. The amount of propellant required to prime was consistent from test to test for the same emitter. Once the emitter was primed, a voltage was applied to the thruster to establish a Taylor cone and fluid jet.

A custom-designed pulsing circuit was used to actuate the Lee microvalve. The emitter priming circuit was designed to produce a 0.5 ms to 50 ms wide voltage pulse. The circuit was composed of four main components, a CMOS NAND gate, a CMOS dual monostable multivibrator, a hex inverting Schmitt trigger, and a power MOSFET optocoupler, which can be seen in Figure 4. When actuated, the NAND gate first removes the chatter from the mechanical switch. With any electromechanical switch there is a fluctuation in the actuation voltage. This removal of the fluctuations is accomplished through two NAND gates. Because the gates have a delay when switched, they do not see the fluctuation.

Once the fluctuations are removed, the clean 5 V signal from the NAND gate output is converted into an inverted square wave by the multivibrator. The pulse width for the circuit is controlled by adjusting the combination of the potentiometer and the capacitor attached to the multivibrator. The inverted square wave that comes out of the multivibrator is cleaned up, inverted, and buffered. This signal actuates the optocoupler, which sends a 5V signal to the emitter-priming valve. The Schmitt trigger is used to increase the drive current to the optocoupler.
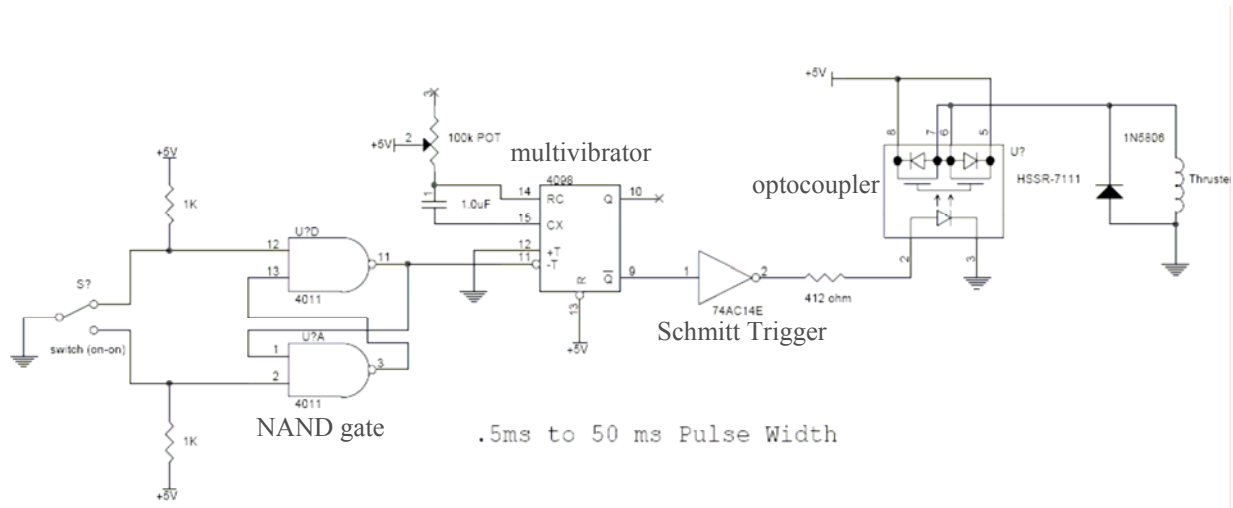
Figure 4. Layout of the priming circuit.

V. Time Of Flight (TOF) Theory

A typical Time Of Flight (TOF) system provides information on a beam's average specific charge or charge-to-mass ratio, q/m. This is done by measuring the time it takes droplets in the spray to move towards a detector. The specific charge of the spray is given in Equation 2 for q/m.[8]

$$\frac{q}{m} = \frac{1}{2(V_N - V_S)}\left(\frac{L}{t_F}\right)^2 \tag{2}$$

The stopping potential is defined as the bias potential at which the current, associated with a given size droplet, reaching the collector has fallen by a factor of a half.[8] V_N is the needle voltage, so the quantity V_N-V_s can be interpreted as the accelerating potential of a droplet. These values must be obtained experimentally in an independent measurement. In the TOF equation, L is the distance between the colloid thruster needle tip and the target and the variable t_F is the time of flight for the droplets to travel the distance L.[8] The thrust (T), and mass flow rate (ṁ) can be calculated from the calculation of q/m and the measured current, I.[9] This is done using equations 3 and 4 and integrating the time of flight spectrum.

$$T = \frac{2V_A}{L} \int_0^\infty \left(\frac{q}{m}\right) I dt \qquad (3)$$

$$\dot{m} = \frac{2V_A}{L^2} \int_0^\infty \left(\frac{q}{m}\right)^2 I dt \qquad (4)$$

VI.   Time of Flight Hardware

The prototype single emitters were tested for performance using a Time Of Flight setup based on these principles. A diagram of the setup is shown here in Figure 5. A 4 kV switch was designed to do the TOF experiment, and an electrometer was also developed that were slightly different from the circuits developed by Gamero *et al*.[8]
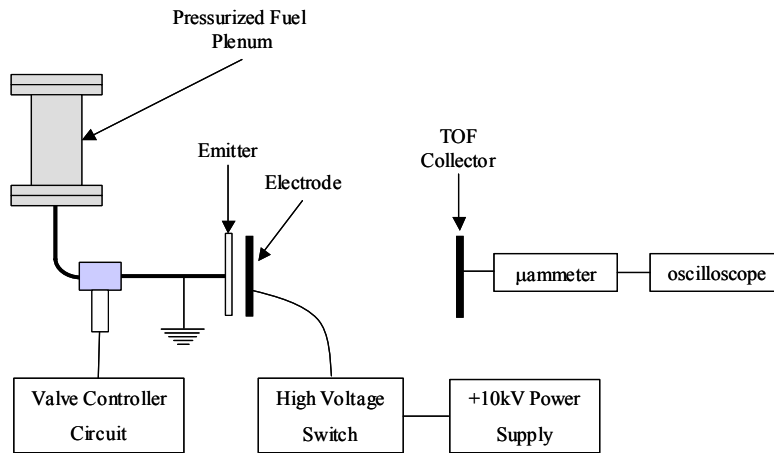
Figure 5. Diagram of the Time Of Flight (TOF) setup.

In order to take data from the time of flight analysis, the emitter voltage must be interrupted by a high-voltage (4 kV), fast-acting (<10μs) switch, as shown in Figure 5. This interruption must have a rapid fall time to ensure accuracy of the collected TOF data. Interruption of the voltage to the emitter allows for a precise point to start the target current collection, which makes up the TOF spectra. The circuit for the switch, shown in Figure 6., was based on a 2 kV switch design by Gamero.[8] The circuit accomplished the rapid fall time through a series of MOSFETS, a voltage divider, and a variable step width signal produced by an external generator. The MOSFET is an N-channel design, which only allows it to switch positive voltage.

A 7 volt pulsed signal was supplied instead of the original 5 V signal to compensate for the 0.7 volt drop across the diodes in series. This ensures that the MOSFET farthest from ground electrically is supplied with at least 4 volts (which is its minimum voltage threshold).

During initial testing of the 4000 V circuit design, a major problem arose causing the 4000 V max to be limited to 2500 V. The problem was caused by the circuit drawing in excess of the power supply's maximum current of 0.015 amps. With the 0.015 current draw, the power supply was limited to a 2,500 volt output. In order to be able to supply 4000 volts, the circuit's current demand was lowered by increasing the resistance of the resistors within the voltage divider. The voltage divider was designed to limit the voltage across each MOSFET to 1000 V. When the voltage was significantly over 1000 V to any one MOSFET within the design, the component burned out.
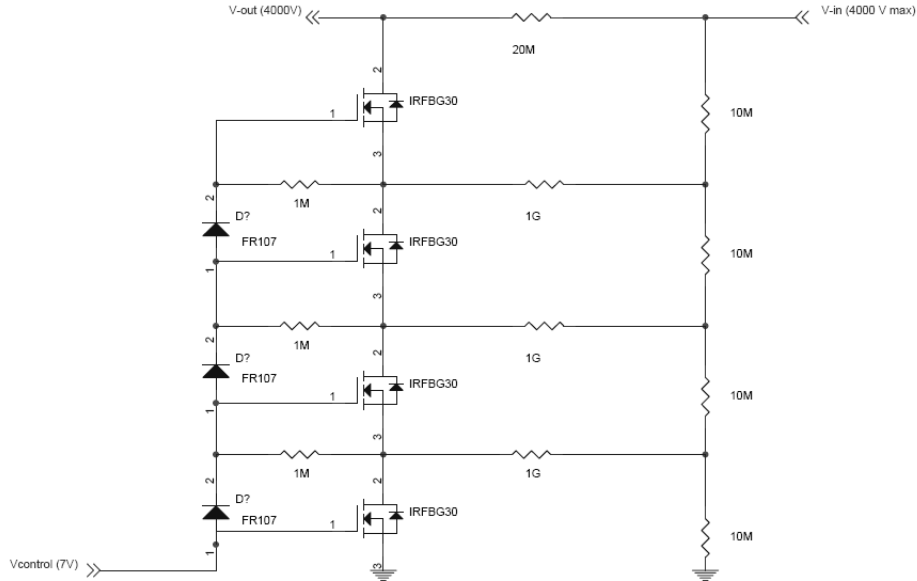
Figure 6. Circuit schematic of the high voltage switch.

The electrometer was also slightly modified from the circuit by Gamero e*t al.*[8] An offset voltage was originally present in the output signal causing the voltage output to be inaccurate by anywhere from 2 to 5 mV. To compensate for the offset, a 10 kΩ multi-turn potentiometer was added to the circuit shown in Figure 7. With the multi-turn potentiometer, the op-amp was trimmed before each test to eliminate the 2-5 mV offset. A Tektronix oscilloscope read out the circuit's conditioned output signal.
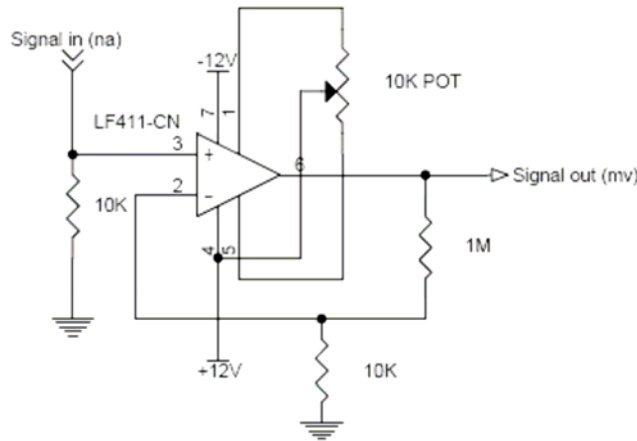
Figure 7. Circuit diagram of the modified microampmeter.

VII.   Results

Normally, the fabrication of the MEMS device prevents optical access to the Taylor cone. A simulated emitter was made to replicate the dimensions of the emitter hole (in stainless steel). This device was not a flat surface around the emitter hole, as it was for the silicon emitter. As was noted previously[4], the flat surface around the emitter hole is not an efficient geometry to amplify the electric field. Thus, the emitter constructed for optical testing was more efficient than the MEMS emitter. Indeed, the formation of the Taylor cone occurred at a much lower voltage (approximately 2200 V) than it did for the MEMS version. An image of the Taylor cone formed with this setup, and captured by the in-vacuum microscope, is shown here in Figure 8.

The 29th International Electric Propulsion Conference, Princeton University,
October 31 – November 4, 2005

Figure 8. Picture of the Taylor cone from the simulated emitter.

An actual emitter was also tested using the setup shown in Figure 5. A TOF time history was collected following an off-step of the 4kV switch. This curve is shown here in Figure 9. Work remains to be done to isolate the obvious noise in the current signal. The current was measured on a nickel plate located 2 cm downstream. The stopping potential of the setup has not been measured.
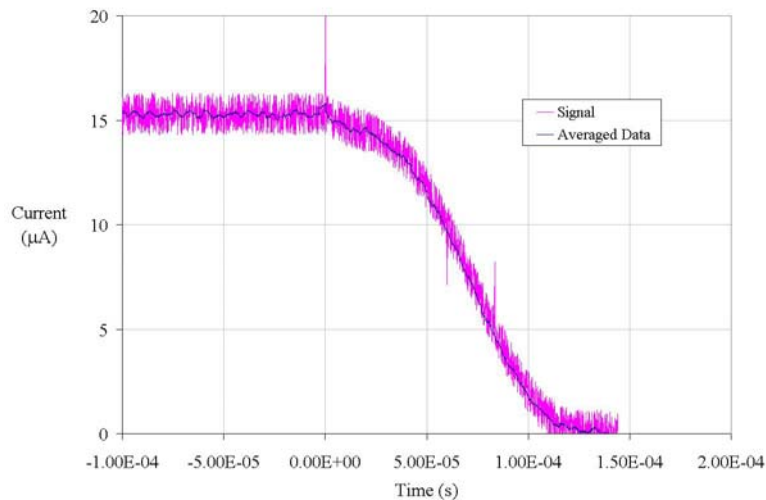
Figure 9. Time Of Flight current after the thruster was switched off at time T=0.

VIII.   Conclusions

Results were obtained for both optical diagnostics of the Taylor cone, and TOF data. Although the data showed the potential of the device for spaceflight, the devices were also found to be highly susceptible to damage from both contamination and contact with the sensitive insulation columns. In the future, the TOF data will be used to characterize the performance of the devices, and the insulation will be improved to reduce the potential for contamination and damage.

The pulsed valve controller enabled the priming of the emitter, but should be combined with a proportional valve for further testing. It is impossible to obtain steady thrust data from the emitter with only the pulsed valve. Two other circuits were also designed and demonstrated, a high-voltage switch, and a microampmeter, that improve the instrumentation designs available for TOF testing.

Acknowledgments

References

[1]Mueller, J., D. Pyle, I. Chakraborty, R. Ruiz, W. Tang, C. Marrese, and R. Lawton, "Electric Breakdown Characteristics of Silicon Dioxide Films for use in Microfabricated Ion Engine Accelerator Grids", Micropropulsion For Small Spacecraft, Edited by M. Micci and A. Ketsdever, *Progress in Astronautics and Aeronautics*, Vol. 187, 2000, pp. 303-334.

[2]Stark, J., B. Kent, R. Stevens, and M. Sandford, "Colloid Propulsion – A Re-evaluation, with an integrated design", AIAA Paper # 2003-4851, 39th AIAA/ASME/ASME/SAE Joint Propulsion Conference, 20-23 July, 2003, Huntsville, AL.

[3]Velasquez, L, J. Carretero, A. Ankinwande, and M. Martinez-Sanchez, "The concept and development of a micro-fabricated colloid thruster array", AIAA paper # 2003-4850, 39th AIAA/ASME/ASME/SAE Joint Propulsion Conference, 20-23 July, 2003, Huntsville, AL.

[4]Cardiff, E., B. Jamieson, P. Norgaard, and A. Chepko, "The NASA GSFC MEMS Colloidal Thruster", AIAA-2004-3592, 40th AIAA/ASME/SAE/ASEE Joint Propulsion Conference and Exhibit, Fort Lauderdale, Florida, July 11-14, 2004.

[5]Zeleny, J., "The Electrical Discharge from Liquid Points, and A hydrostatic method of measuring the electric intensity at their surface", The Physical Review, Vol. III, No. 2, February 1914, pp. 69-91.

[6]Norgren, C. T., and D. S. Goldin, "Experimental Analysis of the Exhaust Beam from a Colloid Thruster", NASA TM X-52035, 1964.

[7]Taylor, G. I., and A. D. McEwan, "The stability of a horizontal fluid interface in a vertical electric field", *J. Fluid Mechanics*, 1965, Vol. 22, Part 1, pp. 1-15.

[8]Gamero-Castaño, M. & Hruby, V. Electric measurements of charged sprays emitted by cone-jets, J. Fluid Mech., 2002, 49, 245-276.

[9]Gamero-Castaño, M. & Hruby, V. Characterization of a colloid Thruster Performing in the micro-Newton Thrust Range. IEPC-01-282, 27th International Electric Propulsion Conference, Pasadena, CA, October 2001.